



Grid Satellite Rainfall Products Potential Application for Developing I-D and E-D Thresholds for Landslide Early Alert System over Bali Island

P. Aryastana

Department of Civil Engineering, Faculty of Engineering and Planning, Warmadewa University,
Denpasar, Indonesia

Email: aryastanaputu@yahoo.com

ARTICLE INFO

Article History :

Article entry : 13 – 02 – 2023
Article revised : 22 – 03 – 2023
Article received : 24 – 04 – 2023

Keywords :

Bali, Landslides, Rainfall,
Satellite, Threshold.

IEEE Style in citing this article:

P. Aryastana, "Grid Satellite Rainfall Products Potential Application for Developing I-D and E-D Thresholds for Landslide Early Alert System over Bali Island," *U Karst*, vol. 7, no. 1, pp. 104 – 118, doi: 10.30737/ukarst.v7i1.4318

ABSTRACT

Bali has been one of the most popular tourist destinations in Indonesia. However, on the other hand, Bali has a high risk of natural disaster vulnerability. The number of landslides in Bali took the first position compared to other natural disasters. Currently, remote sensing platforms can present Grid Satellite Rainfall Products (GSRPs), which provide rainfall information that can identify rainfall conditions for landslide events. This study aims to analyze the potential GSRPs application of Precipitation Estimation from Remotely Sensed Information Using Artificial Neural Networks (PERSIANN), the Integrated Multi-satellite Retrievals for Global Precipitation Measurement (IMERG), and Global Satellite Mapping of Precipitation (GSMaP) in determining the mean rainfall intensities and duration (I-D); accumulated rainfall and duration (E-D) thresholds for landslide occurrences over Bali Island. The method used to develop I-D and E-D thresholds is the power-law equation and frequentist sampling method in various probability levels (5%, 10%, 20%, 30%, 40%, and 50%). The result shows that I-D and E-D thresholds established by GSRPs are generally lower than the threshold defined by rain gauge observations. Among the three GSRPs, IMERG is performing the best in establishing the I-D and E-D thresholds for landslide phenomena. The level of potential that IMERG can use in developing the I-D and E-D thresholds is 59.16% and 84.06%, respectively. The E-D threshold derived from the IMERG product can be used to establish the landslide early alert system over Bali Island because it has a high spatial-temporal resolution, word-wide coverage, and near-real-time observation.

1. Introduction

Bali has been nown as one of the most popular tourist destinations in Indonesia and eworldwide Bali is famous for its natural beauty, cultural diversity, and the hospitality of its people. Bali's beautiful coastal region has white sandy beaches, sea corals, and towering steep cliffs. In the interior, Bali has lush mountains and valleys and many rice fields, plantations, and

Grid Satellite Rainfall Products Potential Application for Developing I-D and E-D Thresholds for Landslide Early Alert System over Bali Island

<https://dx.doi.org/10.30737/ukarst.v7i1.4318>

tropical forests[1]. In addition to its natural beauty, Bali has a fairly high vulnerability to natural disasters due to its complex and heterogeneous regional conditions[2][3]. This heterogeneous region is a challenge in dealing with natural disasters because the types of disasters that occur can vary, such as earthquakes, floods, landslides, and tsunamis[4][5][6]. Landslide events are frequently occurring in Bali. The number of landslides in Bali took the first position in 2017-2019 compared to other natural disasters. Conforming to the World Health Organization in the range from 1998-2017, Landslides impact approximately 4.8 million population and cause more than 18 thousand mortalities [7]. So it becomes a serious problem that must be considered.

Landslides can occur suddenly due to unpredictable triggering factors, such as earthquakes, volcanic eruptions, or other natural events [8]. This trigger factor can cause drastic and sudden soil movement and can trigger landslides in vulnerable areas. However, in general, landslides tend to occur gradually, and there are few signs or symptoms before the occurrence of landslides that can be identified. Landslides that tend to occur gradually are caused by factors that contribute to the stability of slopes or soil in an area. These factors include high and prolonged rainfall, excessive soil moisture, landslide-prone soil types, steep topography, and human activities such as logging and soil mining [9].

The landslide triggered by rainfall is a popular natural hazard regularly occurring around the world [10] [11]. The occurrences of landslides primarily provoked by rainfall infiltration are associated with rainfall duration, rainfall accumulation, and antecedent rain rate, causing a rise in the soil pore pressure so that the shear stress of the soil decreases [12] [13]. To reduce the risk of landslides, early alert systems for forecasting the landslide-triggering amount of rain were established at global and regional scales derived from different procedures and input raw data [14][15]. The prediction of rainfall-generated landslides calculates on physical or empirical approaches.

The physical approach can forecast the failures by examining the terrain information, soil formation, and environmental condition of the study region. In the empirical method, evaluating the possibility of landslide occurrences is determined by analyzing previous rain rate occurrences that initiated landslides. Recently, empirical rainfall thresholds have been used to establish the early alert system of landslide occurrences on a global and regional scale [14]. The frequent rainfall thresholds used on multiple spatial scales are the mean rainfall intensities and duration (I-D) and accumulated rainfall and duration (E-D) thresholds [16]. I-D and E-D thresholds are thresholds that are uncomplicated to operate, deterministic methods, and can be

used to identify critical rainfall values that initiate landslides [17][18]. Hence, the I-D and E-D thresholds are chosen in the current study.

The accuracy of I-D and E-D thresholds is highly dependent on the quality of rainfall data as a primary input [19]. Reliable rainfall data used to define rainfall thresholds are obtained from rain gauge measurements. However, the spatial coverage of rain gauge stations which are very rare in remote areas and high terrain, is a major issue in their use to develop rainfall thresholds for landslide occurrences. Recently, remote sensing platforms have been capable to present global grid satellite rainfall products (GSRPs) at high spatial and temporal resolution. GSRPs have the potential to be used to determine rainfall thresholds for landslide occurrences because it provides global rainfall estimates over remote areas and complex topography and have a high temporal resolution [1]. Some research on the use of GSRPs in determining rainfall thresholds has grown considerably.

The first potential GSRPs used to obtain the global rainfall intensity-duration threshold framework for global landslide occurrences was the use of the Tropical Rainfall Measuring Mission (TRMM) Multi-satellite Precipitation Analysis (TMPA) datasets. Problems in original derivation due to the vulnerability of spatial resolution maps and the need to reanalyze I-D thresholds to assess regional climatology better. Estimation (PERSIANN) to establish a global landslide forecast model. The previous studies highly emphasize the potential of GSRPs in determining rainfall threshold. However, some of the past studies mentioned above only derived I-D and E-D separately, so the current study will analyze both I-D and E-D thresholds using IMERG, GSMaP, and PERSIANN.

The past studies at most analyzed the rainfall occurrences by using 3 hours to daily rainfall dataset, so that in this study analyzes the rainfall occurrences by utilizing the high temporal resolution GSRPs (0.5 hours and 1 hour). Moreover, based on the author's knowledge, there are no previous studies in determining the rainfall threshold for landslide events using either rain gauge data or GSRPs over Bali Island. Therefore, it is important to develop the rainfall thresholds for landslide occurrences in Bali Island by using satellite-based rainfall datasets because the coverage of rain gauge stations in Bali Island is not widespread enough and is limited in the high terrain areas.

This study aims to analyze the potential application of three Global Satellite-Rainfall Products (GSRP), namely PERSIANN, IMERG, and GSMaP, in determining the threshold of rainfall intensity (I-D) and rainfall duration (E-D) for landslide events on the island of Bali. It is expected that from this analysis, satellite data can be found that has the most potential in

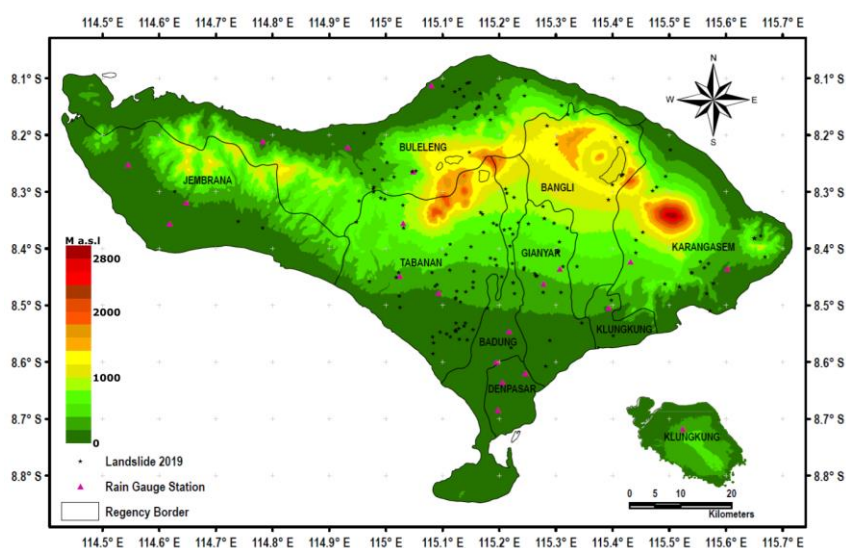
determining rainfall thresholds that can trigger landslides. The data will be used to build a landslide early warning system on the island of Bali.

2. Research Method

The I-D and E-D thresholds for landslide occurrences over Bali Island are determined using PERSIANN, IMERG, dan GSMaP datasets. The main data collected in this study consisted of landslide occurrence data and rain data. The value of the rainfall event before the occurrence of a landslide was determined by finding the average and total rainfall immediately before the occurrence of a landslide for each dataset. The rainfall values and duration distribution for each landslide event is plotted in a scatter diagram with a logarithmic scale. The power-law relationship between rainfall value and duration in various probability levels was used to establish the I-D and E-D thresholds. The details information on the study area, landslide data, rainfall data, and rainfall event-duration analysis are shown in the following subsections:

2.1 Area of study

The study site for determining the I-D and E-D thresholds was in Bali Island (**Figure 1.**). Bali is an Indonesian province enclosed east of Java and west of Lombok Island. It is located 8 degrees below the equator. Bali has a total area of 5620 km² and measures approximately 140 km by 80 km. As a result of its complex terrain and high rains, Bali Archipelago is highly prone to landslides. Bali has a drought period from May to October and a rainy period from November to April, which follows similar seasonal variations as Indonesia.



Source: Author's Compiles (ArcGIS, 2022).

Figure 1. Elevation Map of Bali and Landslide Events Position.

2.2 Landslide Data

The landslide events data is acquired from the Regional Disaster Management Agency of 8 regencies over Bali province. In this study, collected 66 landslide incidents were provoked by rainfall in 2019. The reference details for every landslide consist of the location (village or site) and the time when it happened (hour or date). The latitude and longitude of the landslide events were acquired by field surveying. **Figure 1.** reveals the positions of landslides and the propagation of altitude in Bali.

2.3 Rainfall Data

Two kinds of rainfall datasets were used to determine the rainfall thresholds: (i) rain gauge measurements and (ii) GSRPs (IMERG, GSMaP, and PERSIANN).

1. Gauge-observed precipitation data

Indonesia's BWSBP Ministry of Public Works and Human Settlements provided the hourly rain gauge data. They only can provide 18 hourly rain gauge observation data for the completion in 2019. Because gauge measurements are not frequently near landslide locations, the author chose the 16 rain gauge measurements closest to the site of every incident. Relying on Balai Wilayah Sungai Bali-Penida (BWSBP) rain gauge information from 2015 to 2017, the amount of rain in Bali was defined to be approximately 180 mm/month; the greatest amount of rain happens from December to February, while the minimum amount of rain happens from July to August [1]. Rainfall is the main trigger for landslide events in Bali Province. According to data from the Statistics of Bali Province from 2018 to 2022, the landslide disaster is the first rank occurrence if compared to another disaster.

2. Satellite-based precipitation products

Three GSRPs used are PERSIANN, IMERG, and GSMaP. The IMERG product is accessible online at <https://gpm.nasa.gov/data/directory>. The GSMaP_Gauge version 7 was used in the present study with the one-hour time resolution, 10 km x 10 km pixel size, and is easily downloaded into the JAXA official site (ftp://rainmap:Niskur+1404@hokusai.eorc.jaxa.jp/standard/v7/hourly_G/). In this study, the PERSIANN-CCS dataset with 0.04° spatial resolution and hourly time resolution was used. This dataset is free and accessible at <https://chrsdata.eng.uci.edu/>.

2.4 Rainfall Event-Duration Analysis

The configuration equation that is frequently used for establishing the I-D and E-D thresholds for slope failure occurrences is the power-law correlation, defined as:

$$I = \alpha \cdot D^\beta \quad (1)$$

$$E = \alpha \cdot D^\beta \quad (2)$$

With I is the average rain rate (mm/hour); E is the abundance of rain (mm); D is the period of rainfall occurrences (hour); α is the scaling factor, and β is the slope variable

Based on the above formulation, this study used the frequentist sampling technique to estimate the I-D and E-D thresholds for all GSRPs and gauge measurements. The I-D and E-D thresholds in the present study are determined based on 5%, 10%, 20%, 30%, 40%, and 50% exceedance levels, which means that the probability of a landslide due to rainfall events not exceeding the rainfall thresholds is less than 5%, 10%, 20%, 30%, 40%, and 50%. These probability levels have been widely used to analyze the rainfall threshold for frequentist sampling techniques [16][19].

Two major processes were conducted in the features extraction of rainfall datasets to recognize landslides provoking rainfall occurrences. First, the catalog's landslide coordinates were geographically matched to satellite pixels and rain gauges. The GSRPs recognized the cell containing the landslide induction position, whereas the gauges assumed the single closest neighbor to the landslide position, as is normally accepted in gauge-based landslide-provoking rainfall prediction [20]. Second, the derived data series from every gauge/pixel could be produced to define and classify the rainfall occurrences that caused the landslides. The occurrences that happened mostly on the date of the landslide could be regarded, and a one-day no-rain occurrence was selected as the least interevent period [21]. Several past studies obtained 7 days of antecedent rainfall as an essential factor for initiating landslide occurrences [22]. Hence, the present study further analyzed rainfall total for 7 days (168 hours) before the start of rainfall events that initiated landslide occurrences.

3. Results and Discussions

The I-D and E-D threshold were inferred from the rain gauge, IMERG, GSMaP, and PERSIANN datasets using landslide occurrences during 2019 in Bali Island.

3.1 Rainfall Event Condition

Rainfall data provides an overview of the amount of rain that falls on an area in a certain period. This data can consist of several parameters such as intensity, duration, frequency, cumulative rainfall, and previous rainfall. Rainfall data is described in **Table 1** below:

Table 1. Rainfall Events Conditions

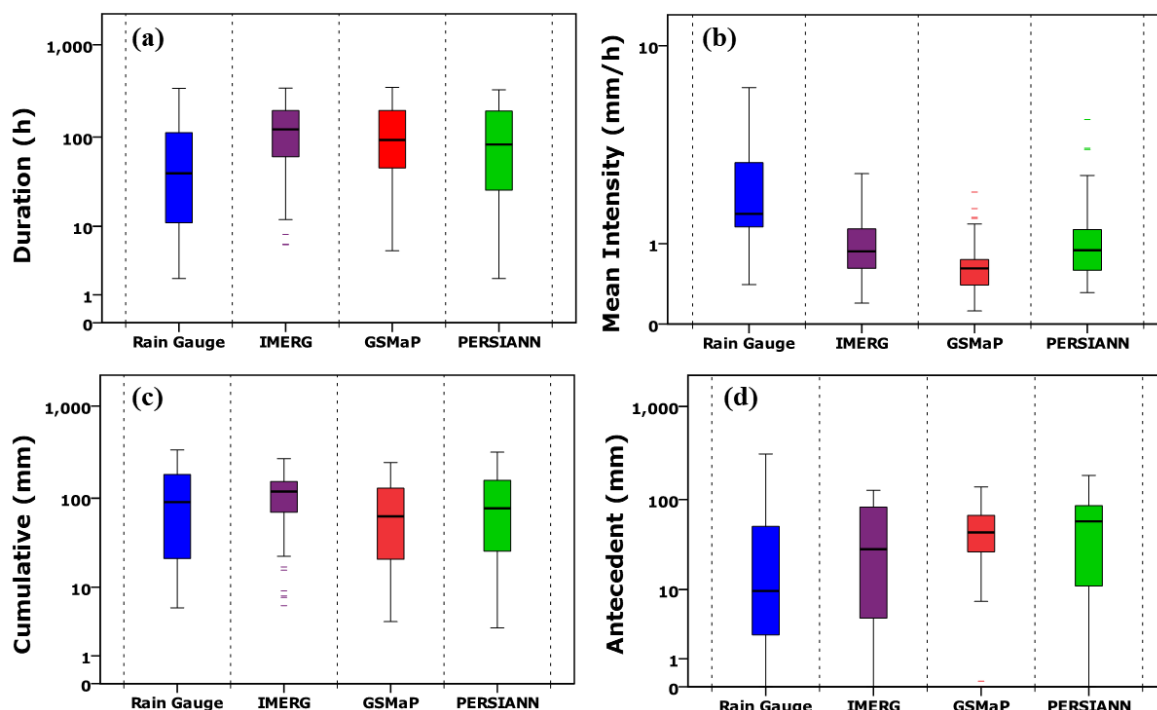
Products	Rainfall condition	Mean Intensity (mm/hour)	Duration (hour)	Cumulative rainfall (mm)	Antecedent rainfall (mm)
Rain Gauge	Average	2.16	64.73	105.80	36.63
	Max.	6.68	339.00	334.30	309.50
	Min.	0.41	2.00	5.60	0.00
IMERG	Average	1.12	132.58	116.26	44.42
	Max.	2.66	341.00	268.95	126.04
	Min.	0.20	6.00	5.97	0.00
GSMaP	Average	0.66	128.20	77.64	53.85
	Max.	2.12	347.00	244.36	136.76
	Min.	0.12	5.00	3.68	0.00
PERSIANN	Average	1.08	114.05	102.24	65.65
	Max.	4.83	326.00	317.00	182.00
	Min.	0.31	2.00	3.00	0.00

Source: Author's Analysis.

From **Table 1**. The mean rainfall intensity indicates all GSRPs exhibited an underestimate of the average rain-rate to provoke landslide events. The underestimation means the mean rainfall intensity produced by GSRPs exhibited lower than the rain gauge. The maximum duration of rainfall occurrences triggering landslides from the gauge, IMERG, GSMaP, and PERSIANN is 339 hours, 341 hours, 347 hours, and 326 hours, respectively. This shows that the duration of rainfall that causes landslides detected by GSRPs and near-approximation rain stations is about 14 days or 2 weeks.

The average rainfall duration of all GSRPs was confirmed higher with rain gauge observation. The maximum cumulative and antecedent rainfall of the rain gauge shows the highest compared to all satellite rainfall datasets. This indicates the satellite rainfall datasets are underestimation in producing the maximum cumulative and antecedent rainfall. The average value of rainfall accumulation triggering landslides for all products reveals more than 75 mm; this indicates that the occurrence of landslides on the island of Bali in 2019 is more likely to be influenced by accumulated rainfall. The range of cumulative rainfall that initiates the landslide occurrences on the rain gauge, IMERG, GSMaP, and PERSIANN is 5.60 mm to 334.30 mm, 5.97 mm to 268.95 mm, 3.68 mm to 244.36 mm, and 3.00 mm to 317.00 mm, respectively.

In addition to **Table 1**, Rainfall events conditions are also presented in graphical form to visualize data in a clearer and easier to understand form. Graphs can provide an overview of the rainfall conditions of each data source, namely stations, and satellites.



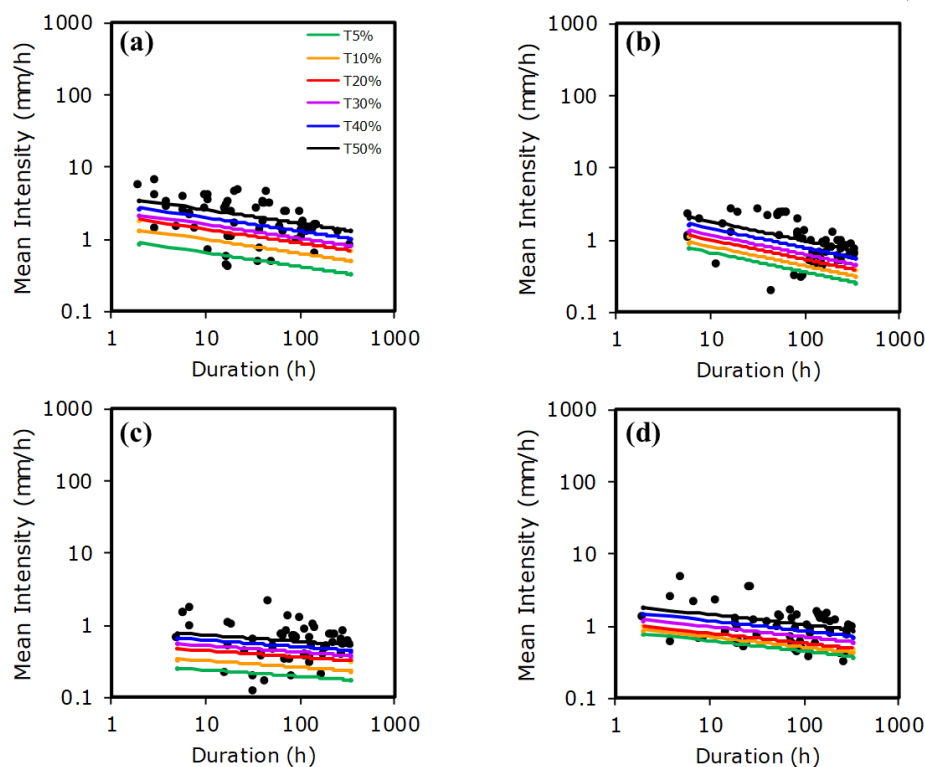
Source: Author's Analysis.

Figure 2. Box Plots of Rainfall Condition: (a) Duration, (b) Mean Rainfall Intensity, (c) cumulative rainfall, and (d) Antecedent Rainfall.

Inspection of **Figure 2. a** reveals that the GSRP's rainfall duration has a long duration compared with the rain gauge duration. **Figure 2. b** shows that all satellite products generally underestimate the mean rainfall intensity that induces landslides measured by the rain gauge. However, the IMERG and PERSIANN show better performance in capturing mean rainfall intensity compared with GSMaP. From **Figure 2. c** the cumulative rainfall for PERSIANN is comparable to that of a rain gauge, while IMERG and GSMaP show overestimate and underestimate, respectively. However, IMERG has a small deviation in capturing rainfall accumulation that initiates landslide events compared to other products. All satellite rainfall datasets depict an overestimated antecedent rainfall (**Figure 2.d**).

3.2 Rainfall Thresholds

In determining rainfall thresholds, it is necessary to determine the appropriate I-D and/or E-D threshold values, which indicate when the risk of a landslide disaster increases significantly. The I-D and E-D thresholds are based on historical data on rainfall and landslide events in the area. An analysis of the relationship between rainfall intensity and the duration at which landslides occur is carried out in determining the I-D threshold. Meanwhile, in determining the E-D threshold, an analysis of the relationship between accumulated rainfall and the duration in which landslides occur is carried out.

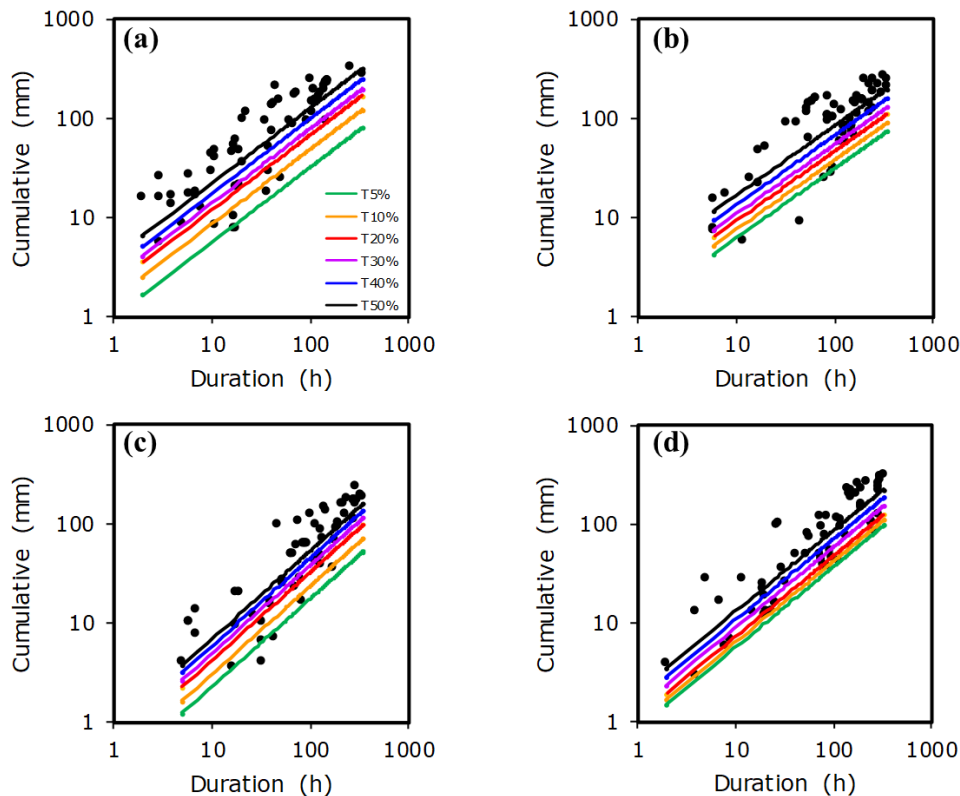


Source: Author's Analysis.

Figure 3. (a) I-D Thresholds for the Rain Gauge. (b) I-D Thresholds for IMERG. (c) I-D Thresholds for GSMaP. (d) I-D Thresholds for PERSIANN.

The probability of every I-D threshold represents the potentiality of landslides when rainfall above the I-D curve happens. As presented in **Figure 3**, the I-D threshold of the GSMaP dataset is lower than other datasets. This shows that the GSMaP dataset has the worse in determining the I-D threshold compared to other datasets. The IMERG threshold is relatively close to the I-D threshold determined by the rain gauge dataset, and this might be due to the highest temporal resolution of the IMERG product. The slope of the PERSIANN demonstrated relatively similar to the rain gauge observation. This is might due to the highest spatial resolution of the PERSIANN dataset. However, the GSMaP rainfall thresholds exhibited the lowest compared to rain gauge, IMERG, and PERSIANN. This result indicates the GSRPs exhibited underestimated I-D threshold compared to the rain gauge observation.

The E-D threshold at exceeding probabilities from 5% to 50% for the rain gauge, IMERG, GSMaP, and PERSIANN datasets are shown in **Figure 4. a**, **Figure 4. b**, **Figure 4. c**, and **Figure 4.d**, respectively.



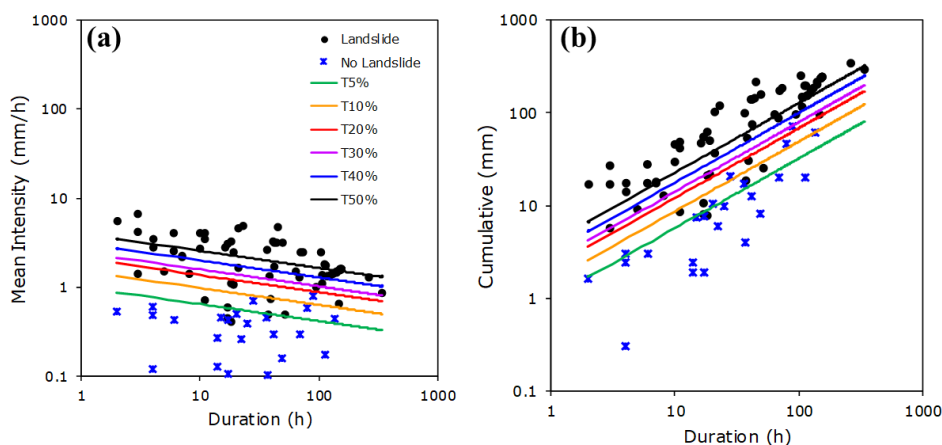
Source: Author's Analysis.

Figure 4. (a) E-D Thresholds for the rain gauge. (b) E-D Thresholds for IMERG. (c) E-D Thresholds for GSMaP. (d) E-D Thresholds for PERSIANN.

The slope of the E-D threshold of all GSRPs is comparable to that of a rain gauge, while the E-D thresholds of the three GSRPs tend to be lower compared to the rain gauge observation. The distribution of rainfall duration that causes landslides in IMERG products is more concentrated over more than 100 days (**Figure 4. b**) compared to evenly distributed rain stations (**Figure 4. c**). All GSRPs produce a lower E-D threshold than those generated from rain stations.

3.3 Verification and Prediction Accuracy

The verification of landslide and no landslide occurrences for I-D and E-D thresholds at different exceeding probabilities are shown in **Figure 5. a** and **Figure 5. b**, respectively. Based on the verification results reveal, most of the landslide events occur above the I-D lines for a probability of 20% (red line in **Figure 5. a**). This indicates the probability of landslide occurrences provoked by rainfall not exceeding the rainfall threshold is less than 20%. On the other hand, most of the landslide events occur above the E-D lines for a probability of 30% (purple line in **Figure 5. b**). This means the likelihood of landslides caused by rainfall that does not reach the rainfall threshold is below 30%.



Source: Author's Analysis.

Figure 5. (a) Verification Landslide and No Landslide for I-D Threshold. (b) Verification Landslide and No Landslide for E-D Threshold.

The I-D and E-D thresholds equation derived from the rain gauge and GSRPs over Bali Island is tabulated in **Table 2**. **Table 2** also demonstrates the relative differences of the threshold parameters in estimating mean rainfall intensity, cumulative rainfall, and rainfall duration. The differences between the GSRP's threshold variables from the rain gauge threshold variables are within 75% (75.10%), with some datasets showing differences lower than 10% (6.91%). All GSRPs underestimate the intercept parameter (α), while for the slope parameter (β), the IMERG dataset overestimates the I-D thresholds. The slope parameter of the E-D thresholds indicates that the IMERG underestimates, while both GSMaP and PERSIANN overestimate. The GSMaP has the largest deviation of all threshold variables (α and β) compared to other GSRPs. Among the three GSRPs, IMERG has the lowest relative deviation of α compared with other datasets. PERSIANN dataset exhibited better accuracy of β in the I-D threshold, while IMERG demonstrated better performance in the E-D threshold.

Table 2. Rainfall Threshold Equation and Relative Differences of Intercept and Slope Parameters to the Rain Gauge.

Threshold	Dataset	Equation	The relative deviation of α (%)	The relative deviation of β (%)
I-D	Rain Gauge	$I = 2.126 \cdot D^{-0.191}$	0.00	0.00
	IMERG	$I = 1.860 \cdot D^{-0.269}$	-15.94	40.84
	GSMaP	$I = 0.551 \cdot D^{-0.091}$	-75.10	-52.36
	PERSIANN	$I = 1.108 \cdot D^{-0.141}$	-49.92	-26.18
E-D	Rain Gauge	$E = 2.126 \cdot D^{0.753}$	0.00	0.00
	IMERG	$E = 1.860 \cdot D^{0.701}$	-15.94	-6.91
	GSMaP	$E = 0.551 \cdot D^{0.886}$	-75.10	17.66
	PERSIANN	$E = 1.108 \cdot D^{0.817}$	-49.92	8.50

Source: Author's Analysis.

The IMERG dataset has the relative deviation of α and β of 15.94% and 40.84% for the I-D threshold, respectively (**Table 2**). This indicates that the IMERG dataset can potentially be used in developing an I-D threshold of 59.16%. On the other hand, the IMERG dataset still has an uncertainty level of 40.84%. In addition, **Table 2** also depicts the relative difference of slope and intercept parameters for the E-D threshold is 6.91% and 15.94%, respectively. This means that the level error of the IMERG dataset in determining the E-D threshold is 15.94%, or the level of potential that IMERG can use in establishing the E-D threshold is 84.06%.

3.5 Potential Application of IMERG

The accuracy analysis shows that the IMERG dataset outperformed other GSRPs in determining the rainfall threshold for landslide occurrences. The accuracy of IMERG in determining the I-D and E-D thresholds is 59.16% and 84.06%, respectively, based on The relative deviation of slope (β) and intercept parameters (α) (**Table 2**). This indicates the IMERG dataset has a high possibility for determining the E-D threshold. However, there is still a 15.94% uncertainty that might be due to the discrepancies in spatial projection and rainfall sampling [23][24][25]. The E-D threshold derived from the IMERG dataset was potentially used to establish the landslide early alert system over Bali Island. The uncertainty correction and integration of the IMERG dataset and hourly rain gauge measurement are required before applying to the landslide early alert system.

4. Conclusion

The I-D and E-D thresholds established by GSRPs are generally lower than the threshold defined by rain gauge observations. Among the three GSRPs, IMERG is performing the best in determining the rainfall threshold for landslide occurrences. The level of potential that IMERG can use in developing the I-D and E-D thresholds is 59.16% and 84.06%, respectively. The E-D threshold derived from the IMERG product can be used to establish the landslide early alert system over Bali Island because it has high spatial-temporal resolution, word-wide coverage, and near-real-time observation.

References

- [1] C.-Y. Liu, P. Aryastana, G.-R. Liu, and W.-R. Huang, "Assessment of satellite precipitation product estimates over Bali Island," *Atmos. Res.*, vol. 244, p. 105032, Nov. 2020, doi: 10.1016/j.atmosres.2020.105032.
- [2] J. J. Wellik, S. G. Prejean, and D. K. Syahbana, "Repeating Earthquakes During Multiple Phases of Unrest and Eruption at Mount Agung, Bali, Indonesia, 2017," *Front. Earth Sci.*, vol. 9, no. May, pp. 1–11, 2021, doi: 10.3389/feart.2021.653164.
- [3] I. K. A. Putra and I. G. Wardika, "Analisis Kerentanan Lahan Terhadap Potensi Bencana Tanah Longsor pada Wilayah Kaldera Batur Purba," *Media Komun. Geogr.*, vol. 22, no. 2, p. 208, 2021, doi: 10.23887/mkg.v22i2.36925.
- [4] S. Hall *et al.*, "Tsunami knowledge, information sources, and evacuation intentions among tourists in Bali, Indonesia," *J. Coast. Conserv.*, vol. 23, no. 3, pp. 505–519, 2019, doi: 10.1007/s11852-019-00679-x.
- [5] Z. Zulfakriza *et al.*, "Tomographic Imaging of the Agung-Batur Volcano Complex, Bali, Indonesia, From the Ambient Seismic Noise Field," *Front. Earth Sci.*, vol. 8, no. February, pp. 1–11, 2020, doi: 10.3389/feart.2020.00043.
- [6] M. T. Gunawan *et al.*, "Analysis of swarm earthquakes around Mt. Agung Bali, Indonesia prior to November 2017 eruption using regional BMKG network," *Geosci. Lett.*, vol. 7, no. 1, 2020, doi: 10.1186/s40562-020-00163-7.
- [7] WHO, "Landslides."
- [8] Y. Wu, Y. Ke, Z. Chen, S. Liang, H. Zhao, and H. Hong, "Application of alternating decision tree with AdaBoost and bagging ensembles for landslide susceptibility mapping," *Catena*, vol. 187, no. October 2019, p. 104396, 2020, doi: 10.1016/j.catena.2019.104396.
- [9] T. Lei, Y. Zhang, Z. Lv, S. Li, S. Liu, and A. K. Nandi, "Landslide Inventory Mapping From Bitemporal Images Using Deep Convolutional Neural Networks," *IEEE Geosci. Remote Sens. Lett.*, vol. 16, no. 6, pp. 982–986, 2019, doi: 10.1109/LGRS.2018.2889307.
- [10] M. Hong, J. Kim, and S. Jeong, "Rainfall intensity-duration thresholds for landslide prediction in South Korea by considering the effects of antecedent rainfall," *Landslides*, vol. 15, no. 3, pp. 523–534, Mar. 2018, doi: 10.1007/s10346-017-0892-x.
- [11] R. A. Yuniawan *et al.*, "Revised Rainfall Threshold in the Indonesian Landslide Early Warning System," *Geosciences*, vol. 12, no. 3, p. 129, Mar. 2022, doi: 10.3390/geosciences12030129.

- [12] N. Rahmawati, "Space-time variogram for daily rainfall estimates using rain gauges and satellite data in mountainous tropical Island of Bali, Indonesia (Preliminary Study)," *J. Hydrol.*, vol. 590, no. June 2020, p. 125177, 2020, doi: 10.1016/j.jhydrol.2020.125177.
- [13] S. W. Kim, K. W. Chun, M. Kim, F. Catani, B. Choi, and J. Il Seo, "Effect of antecedent rainfall conditions and their variations on shallow landslide-triggering rainfall thresholds in South Korea," *Landslides*, vol. 18, no. 2, pp. 569–582, Feb. 2021, doi: 10.1007/s10346-020-01505-4.
- [14] S. Segoni *et al.*, "Technical Note: An operational landslide early warning system at regional scale based on space–time-variable rainfall thresholds," *Nat. Hazards Earth Syst. Sci.*, vol. 15, no. 4, pp. 853–861, Apr. 2015, doi: 10.5194/nhess-15-853-2015.
- [15] L. Piciullo *et al.*, "Definition and performance of a threshold-based regional early warning model for rainfall-induced landslides," *Landslides*, vol. 14, no. 3, pp. 995–1008, Jun. 2017, doi: 10.1007/s10346-016-0750-2.
- [16] S. He, J. Wang, and S. Liu, "Rainfall Event–Duration Thresholds for Landslide Occurrences in China," *Water*, vol. 12, no. 2, p. 494, Feb. 2020, doi: 10.3390/w12020494.
- [17] W. Y. Lee, S. K. Park, and H. H. Sung, "The optimal rainfall thresholds and probabilistic rainfall conditions for a landslide early warning system for Chuncheon, Republic of Korea," *Landslides*, vol. 18, no. 5, pp. 1721–1739, May 2021, doi: 10.1007/s10346-020-01603-3.
- [18] S. Segoni, S. L. Gariano, and A. Rosi, "Preface to the Special Issue 'Rainfall Thresholds and Other Approaches for Landslide Prediction and Early Warning,'" *Water*, vol. 13, no. 3, p. 323, Jan. 2021, doi: 10.3390/w13030323.
- [19] M. T. Brunetti, M. Melillo, S. Peruccacci, L. Ciabatta, and L. Brocca, "How far are we from the use of satellite rainfall products in landslide forecasting?," *Remote Sens. Environ.*, vol. 210, pp. 65–75, Jun. 2018, doi: 10.1016/j.rse.2018.03.016.
- [20] E. I. Nikolopoulos, S. Crema, L. Marchi, F. Marra, F. Guzzetti, and M. Borga, "Impact of uncertainty in rainfall estimation on the identification of rainfall thresholds for debris flow occurrence," *Geomorphology*, vol. 221, pp. 286–297, Sep. 2014, doi: 10.1016/j.geomorph.2014.06.015.

- [21] E. I. Nikolopoulos, E. Destro, V. Maggioni, F. Marra, and M. Borga, “Satellite rainfall estimates for debris flow prediction: An evaluation based on rainfall accumulation-duration thresholds,” *J. Hydrometeorol.*, vol. 18, no. 8, pp. 2207–2214, 2017, doi: 10.1175/JHM-D-17-0052.1.
- [22] C.-W. Chen, H. Saito, and T. Oguchi, “Rainfall intensity–duration conditions for mass movements in Taiwan,” *Prog. Earth Planet. Sci.*, vol. 2, no. 1, p. 14, Dec. 2015, doi: 10.1186/s40645-015-0049-2.
- [23] F. Marra, E. I. Nikolopoulos, J. D. Creutin, and M. Borga, “Radar rainfall estimation for the identification of debris-flow occurrence thresholds,” *J. Hydrol.*, vol. 519, pp. 1607–1619, Nov. 2014, doi: 10.1016/j.jhydrol.2014.09.039.
- [24] E. I. Nikolopoulos, M. Borga, J. D. Creutin, and F. Marra, “Estimation of debris flow triggering rainfall: Influence of rain gauge density and interpolation methods,” *Geomorphology*, vol. 243, pp. 40–50, Aug. 2015, doi: 10.1016/j.geomorph.2015.04.028.
- [25] E. Destro, F. Marra, E. I. Nikolopoulos, D. Zoccatelli, J. D. Creutin, and M. Borga, “Spatial estimation of debris flows-triggering rainfall and its dependence on rainfall return period,” *Geomorphology*, vol. 278, pp. 269–279, Feb. 2017, doi: 10.1016/j.geomorph.2016.11.019.